

# Research Journal of Pharmaceutical, Biological and Chemical Sciences

## Physico-chemical studies, indirect band gap energy and antitumor assay of some selected oxaloyldihydrazones and their cobalt(II) complexes.

Ayman H. Ahmed<sup>1,2\*</sup>, Ali M. Hassan<sup>2</sup>, Hosni A. Gumaa<sup>2</sup>, Bassem H. Mohamed<sup>2</sup>,  
Ahmed M. Eraky<sup>2</sup>, and Ahmed A. Omran<sup>2</sup>.

<sup>1</sup>Chemistry Department, College of Science and Arts, Al-Jouf University, Al Qurayat, Saudi Arabia.

<sup>2</sup>Department of Chemistry, Faculty of science, Al-Azhar University, Nasr City, Cairo, Egypt.

### ABSTRACT

Series of oxaloyldihydrazone ligands were prepared essentially by the usual condensation reaction of oxaloyldihydrazide with different aldehydes e.g., salicylaldehyde, 2-hydroxy-1-naphthaldehyde, 2-hydroxyacetophenone and 2-methoxy-benzaldehyde in 1:2 molar ratio. The formed compounds were purified to give bis(salicylaldehyde), bis(2-hydroxy-1-naphthaldehyde), bis(2-hydroxyacetophenone) and bis(2-methoxy-benzaldehyde)oxaloyldihydrazone ( $L_1$ ,  $L_2$ ,  $L_3$  and  $L_4$ ), respectively. The structures of the hydrazones ( $L_1$ - $L_4$ ) and their relevant solid cobalt(II) complexes have been ascertained on the basis of data obtained from elemental analyses, spectral UV-Vis., IR, ESR, mass and  $^1\text{H}/^{13}\text{C}$  NMR measurements, magnetism at different temperatures and thermal (TG) analysis. The dihydrazones coordinate to the metal center forming mononuclear complexes with  $L_1$  and  $L_4$  in addition to binuclear complexes with  $L_2$  and  $L_3$ . The cobalt ion preferred octahedral configuration upon chelation. Variation of magnetic susceptibility with temperature referred to the conversion of Co(II) complexes under the effect of heat/oxygen to analogous Co(III) complexes. The band gap energy values of all compounds are characteristic of semiconductor materials. The investigated complexes were assayed for their antitumor activities against the human breast cancer cells (MCF-7). The results suggested that the synthesized Co(II) complexes possess growth inhibition activities. Further, the toxicity of Co(II)- $L_3$ ,  $L_4$  towards the African Green Monkey Kidney cells (VERO cells) were checked.

**Keywords:** Cobalt(II)-oxaloyldihydrazone; Spectroscopic studies; Anti-cancer activity.

*\*Corresponding author*

## INTRODUCTION

Despite hydrazones have been under study for a long time owing to their easy preparation, much of their basic chemistry remains unexplored. Hydrazones and their derivatives constitute a versatile class of organic compounds that are important for drug design, organocatalysis, synthesis of heterocyclic compounds, in addition, they find use as plasticizers, polymerization inhibitors and antioxidants [1]. In the field of analytical chemistry, hydrazones have been extensively used in detection and determination of several metals such as the micro determination of gold by N-cyanoacetylaldehyde hydrazone [2], lanthanides by aryl hydrazones [3], and molybdenum by 2,4-dihydroxy acetophenonebenzoylhydrazone [4]. Some hydrazones are also used in photometric determination of sub-nanograms level of cobalt(II) [5] and extraction of cobalt(II) ions [6,7]. In the context of complexation, hydrazones played a central role in the development of coordination chemistry. Hydrazones obtained by the condensation of 2-hydroxy or methoxy aldehydes and ketones with hydrazides are considered potential polynucleating ligands because they have amide, azomethine and phenol or methoxy functions thus offer a variety of bonding possibilities in metal complexes [8]. Extensive studies have revealed that the lone pair on trigonally hybridized nitrogen atom of the azomethine group is responsible for the chemical and biological activities [9-14], compounds of this type have a great biological activity as anti-tumoral and antiviral agents [12,13]. Nevertheless, a lot of hydrazone-complexes [M= Cu(II), Ni(II), Pd(II), Co(II), Mn(II), V(IV), and Ru(II)] have been studied [11], little complexes of oxaloyldihydrazones have been identified [11, 14-16]. This because oxaloyldihydrazones are soluble only in high polar solvents as dimethylformamide (DMF) and dimethylsulfoxide (DMSO) and this requires much effort to isolate them or their complexes in pure form. So, isolation of such compounds in single crystals will definitely be a difficult task. Worthy mention, some hydrazone complexes have been synthesized in zeolite-Y and the resulting materials were inferred by various physicochemical characterization techniques [17]. In fact hydrazones play an important role in improving the anti-tumor selectivity and toxicity profile of anti-tumor agents by forming drug carrier systems employing suitable carrier proteins [18]. The inhibitory effects of end-to-end thiocyanato-bridged zig-zag polymers of Cu(II), Co(II) and Ni(II) complexes of N'-(1-(pyridin-2-yl)ethylidene)acetohydrazide ligand, on human cell cancer such as lung carcinoma cells (A549 cells), human colorectal carcinoma cells (COLO 205 cells and HT-29 cells), and human hepatocellular carcinoma cells (PLC5 cells) have been studied and revealed that the Cu(II) complexes have the strongest population growth inhibition of human colorectal carcinoma cells (COLO 205 cells and HT-29 cells) [19]. Recent studies pointed out that Co(II)-hydrazones complexes have wide applications as anti-tumor [19], anti-microbial activity [20] and anti-inflammatory [21].

In view of the importance of oxaloyldihydrazones and their chelates, we have undertaken the synthesis of four structures of ligands including bis(salicylaldehyde)oxaloyldihydrazone (L<sub>1</sub>), bis(2-hydroxy-1-naphthaldehyde)oxaloyldihydrazone (L<sub>2</sub>), bis(2-hydroxyacetophenone)oxaloyldihydrazone (L<sub>3</sub>), bis(2-methoxybenzaldehyde)oxaloyldihydrazone (L<sub>4</sub>). The ligands (L<sub>3</sub> & L<sub>4</sub>) are one of the newly compounds, first synthesized in Ref. 14, and subsequently their cobalt complexes have not been isolated or characterized before. The coordination behavior of Co(II) ions towards the above mentioned ligands was studied in comparison among them. Further, the optical band gap energies for all isolated compounds were determined to evaluate their conductivities and describe their optical properties. Finally, the anti-tumor activity of the complexes against breast carcinoma cells as well as the toxicity of the highest inhibitory activity complexes toward the African Green Monkey Kidney (VERO cells) have been investigated to show the possibility for their uses in pharmaceutical industry.

## EXPERIMENTAL

### Materials and physical methods

The selected metal salts, diethyl oxalate, hydrazine monohydrate were purchased from Sigma-Aldrich. The employed aldehydes were of E-Merck grade. Oxalic dihydrazide was prepared by the recipe described in Ref. 11, (Exp/Lit. m.p = 240/240 °C). Other chemicals and solvents were of highest purity and used without further purification. Elemental analyses (CHNM), spectral (UV-Vis., FT-IR, mass) and thermal (TG) measurements were carried out as reported [22,11]. The NMR spectra were recorded on a Varian mercury VX-300 NMR spectrometer. <sup>1</sup>H spectra were run at 300 MHz and <sup>13</sup>C spectra were run at 75.46 MHz in dimethylsulphoxide (DMSO-d<sub>6</sub>). Tetramethylsilane (TMS) was used as an internal reference and chemical shifts are quoted in δ (ppm). The ESR spectra of the powdered Co(II) samples were carried out on Bruker-EMX-(X-bands-9.7 GHz) spectrometer with 100 KHZ frequency, microwave power 1.008 mW and

modulation/amplitude of 4 GAUSS at national center for radiation research and technology, Egypt. Magnetic susceptibility of the samples was measured at different temperatures (300–600 °K) using Faraday's method where a very small quantity of sample was inserted at the point of maximum gradient (maximum force). The temperature of the samples was measured using T-type thermo-couple with junction near the sample to avoid the temperature gradient. The sample is placed in a magnetic field that has a gradient in the vertical direction and the force acting on the sample is determined by using a sensitive balance. The energy (U) of a sample of mass m and magnetic susceptibility  $\chi$  when kept in horizontal magnetic field H is given by

$$U = -\frac{m\chi H^2}{2}$$

The vertical force  $F_z$  exerted on this sample is then given by

$$F_z = m\chi \left( H \frac{dH}{dz} \right)$$

$$F_z = \Delta mg$$

Where  $\Delta m$  is the extra mass measured by the balance due to the force exerted by the field gradient, and g is the acceleration due to gravity (980). The mass susceptibility  $\chi$  of the sample is given by

$$\chi = \frac{\Delta m g}{mH(dH/dz)} \quad \text{cgs units}$$

$$\chi_m = \chi \times M.wt$$

$$\begin{array}{ll} H = 1340 \quad \text{at} \quad I = 4A & (dH / dz) = 173.3 \quad \text{at} \quad I = 4A \\ H = 1990 \quad \text{at} \quad I = 6A & (dH / dz) = 248.8 \quad \text{at} \quad I = 6A \end{array}$$

Where: M.wt is the molecular weight of the sample,  $\Delta m$  is the measured pull, m is the sample weight, g is the acceleration due to gravity and H is the coercive field.

The optical band gap energy ( $E_g$ ) of solids was calculated from Tauc's equations [23,24] demonstrated later.

## Preparations

### Preparation of oxaloyldihydrazone ligands

The dihydrazone ligands; bis(salicylaldehyde)oxaloyldihydrazone ( $L_1$ ), bis(2-hydroxy-1-naphthaldehyde)oxaloyldihydrazone ( $L_2$ ), bis(2-hydroxyacetophenone) oxaloyldihydrazone ( $L_3$ ) and bis(2-methoxybenzaldehyde)oxaloyldihydrazone ( $L_4$ ); were prepared using the same procedure reported in Ref. 11 as follows. Oxalicydihydrazide (0.01 mol) dissolved first in hot water (20 cm<sup>3</sup>) followed by adding methanol (40 cm<sup>3</sup>) was mixed with selected aldehyde [salicylaldehyde, 2-hydroxy-1-naphthaldehyde, 2-hydroxyacetophenone and 2-methoxybenzaldehyde] (0.02 mol) in absolute methanol. The resulting mixture was refluxed for 3 hrs under constant stirring. The product separated out on concentrating the solution to half of its volume and cooling. The fine crystals of the desired ligand was collected by filtration through a Buchner funnel and dried in the oven at 50 °C for 2 h. After that the ligand was recrystallized from DMF-MeOH<sub>aq</sub> mixed solvent, collected, washed thoroughly on filter paper by acetone to remove any excess of DMF and then dried in an electric oven at 50 °C for 4 h. The authenticity of the ligands was proved by elemental analyses as well as IR, mass and NMR spectroscopy (Tables 1,2).

### Preparation of solid complexes

Cobalt(II) complexes were synthesized by the recipe reported in literature [11]. The dihydrazone ligand (1 mmol) was dissolved in a minimum amount of DMF (20 ml) and then 50 ml methanol was added. The resulting solution was added slowly to a methanolic solution of Co(II) acetate. The obtained mixture was heated under reflux for 3 hrs and then reduced to 15 cm<sup>3</sup> by evaporation on hot plate. The resulting reaction mixture was cooled down to room temperature and the colored solid complexes were filtered off, washed several times with successive portions of hot solvents (DMF, methanol and acetone, respectively) to remove any excess of unreacted part of ligand and finally dried in an electric furnace at 80 °C for 5 hrs.

### Methods of anti-tumor evaluation

Human breast cancer (MCF-7) cells were obtained from the American type culture collection (ATCC, ROCKVILLE, MD). The cells were grown on RPMI-1640 medium supplemented with 10 % inactivated fetal calf serum and 50 µg/ml gentamycin. The cells were maintained at 37 °C in a humidified atmosphere with 5 % CO<sub>2</sub> and were subcultured two to three times a week. The anti-tumor activity was evaluated on MCF-7 cells. The cells were grown as monolayers in growth RPMI-1640 medium supplemented with 10 % inactivated fetal calf serum and 50 µg/ml gentamycin. The monolayers of 10,000 cells adhered at the bottom of the wells in a 96-well microtiter plate incubated for 24 hrs at 37 °C in a humidified incubator with 5 % CO<sub>2</sub>. The monolayers were then washed with sterile phosphate buffered saline (0.01 M, pH 7.2) and simultaneously the cells were treated with 100 µl from different dilutions of the test sample in fresh maintenance medium and incubated at 37 °C. A control of untreated cells was made in the absence of the test sample. Six wells were used for each concentration of the test sample. Every 24 hr the observation under the inverted microscope was made. The number of the surviving cells was determined by staining the cells with crystal violet [26] followed by the cell lysine using 33 % glacial acetic acid and read the absorbance at 490 nm using ELISA reader (SunRise, TECAN, INC, USA) after well mixing. The absorbance values from untreated cells were considered as 100 % proliferation. The number of viable cells was determined using ELISA reader as previously mentioned before and the percentage of viability was calculated as  $[1 - (OD_t/OD_c)] \times 100 \%$  where OD<sub>t</sub> is the mean optical density of wells treated with the test sample and OD<sub>c</sub> is the mean optical density of the untreated cells. The 50 % inhibitory concentration (IC<sub>50</sub>) was estimated from graphic plots.

## RESULTS AND DISCUSSION

Oxaloyldihydrazones (L<sub>1</sub>-L<sub>4</sub>) and their solid Co(II)-complexes have been isolated in pure form. The entity of the investigated ligands was authenticated earlier in Refs. 14 and 15 but mentioned here in comparison with their metal complexes. Physical, analytical and spectroscopic data of the hydrazones and their isolated metal complexes are given in Tables 1,2. The complexes are air stable for long time, insoluble in MeOH/EtOH, Et<sub>2</sub>O, CHCl<sub>3</sub>, acetone, CCl<sub>4</sub> as well as benzene. Complexes I, II are soluble in DMF and DMSO while complexes III, IV are partially soluble. Comparison of the elemental analysis for both the calculated and found percentages indicates that the compositions of the isolated complexes coincide well with the proposed formulae.

### Chemical structures of dihydrazones and Co<sup>II</sup>-complexes.

#### IR Spectra and bonding

The positions of the significant IR bands of dihydrazones and their cobalt complexes are registered in Table 2.

**Ligands:** oxaloyldihydrazones (L<sub>1</sub>-L<sub>4</sub>) can exist either in the trans (staggered) configuration or cis-configuration, Fig.1, [11]. In cis- configuration, the dihydrazone can adopt either anti-cis-configuration or syn-cis-configuration. Infrared spectra showed strong bands at 1600-1621 cm<sup>-1</sup> assignable to the azomethine group (ν<sub>C=N</sub>). The observation of these bands confirmed the interaction of dihydrazides with aldehydes forming azomethine linkages. The bands of ν(OH)<sub>phenolic/naphthoic</sub>, ν(NH) and ν(C=O) for L<sub>1</sub>-L<sub>3</sub> were noticed at (3149, 3204 and 1666), (3476, 3166 and 1705(m) +1660(v.s)) and (3448, 3293 and 1689(m) +1651(v.s)) cm<sup>-1</sup>, respectively. Meanwhile,

**Table 1: Analytical, physical and spectroscopic data of the oxaloyldihydrazones and their related cobalt complexes.**

Compd./ symbol	M.p(°C) Color	Found(calcd.)%				<sup>1</sup> H-NMR Chemical shift (δppm)	μ <sub>eff.</sub>	M <sup>+</sup> Found/calcd.	E <sub>g</sub> (eV)	g <sup>⊥</sup>	g <sub>//</sub>	g <sub>av</sub>
		C	H	N	M							
C <sub>16</sub> H <sub>14</sub> N <sub>4</sub> O <sub>4</sub> / L <sub>1</sub>	>300 Yellow	59.1 (58.9)	5.1 (4.3)	16.3 (17.2)	-	12.6(NH, s), 10.98(OH, s), 8.75(CH=N, s), 6.6-8.40 (aromatic protons, m)	-	326.0/ 326.0	2.88	-	-	-
C <sub>24</sub> H <sub>18</sub> N <sub>4</sub> O <sub>4</sub> / L <sub>2</sub>	>300 Yellow	68.1 (67.7)	5.6 (4.3)	12.9 (13.2)	-	12.76(NH, s), 12.57(OH, s), 9.74(CH=N, s), 7.0-8.8 (aromatic protons, m)	-	427.1/426.4	2.46	-	-	-
C <sub>18</sub> H <sub>18</sub> N <sub>4</sub> O <sub>4</sub> / L <sub>3</sub>	>300 Pale Yellow	59.5 (61)	6.1 (5.1)	14.9 (15.8)	-	12.85(NH, s), 11.85(OH, s), 6.6-8.0(aromatic protons, m), 2.48(CH <sub>3</sub> , s)	-	356.4/354.2	2.78	-	-	-
C <sub>18</sub> H <sub>18</sub> N <sub>4</sub> O <sub>4</sub> / L <sub>4</sub>	>300 White	59.2 (61)	5.8 (5.1)	15.7 (15.8)	-	12.3(NH, s), 11.9(OH, s), 8.95(CH=N, s), 6.8-8.5(aromatic protons, m), 3.93(OCH <sub>3</sub> , s)	-	355.0/354.4	3.05	-	-	-
[Co(L <sub>1</sub> -2H)(H <sub>2</sub> O) <sub>2</sub> ].2H <sub>2</sub> O/ I	>300 Re. Brown	41.9 (42.2)	4.3 (4.4)	12.0 (12.3)	12.9 (12.9)	-	4.8	-	2.03	2.05	2.40	2.16
Co <sub>2</sub> (L <sub>2</sub> -3H)(OAc)(H <sub>2</sub> O) <sub>6</sub> / II	>300 Re. Brown	43.7 (44.1)	4.1 (4.3)	7.7 (7.9)	16.2 (16.6)	-	4.6	-	2.08	2.05	2.23	2.11
[Co <sub>2</sub> (L <sub>3</sub> -3H)(H <sub>2</sub> O) <sub>6</sub> ].OAc/ III	>300 Red	37.2 (37.7)	4.3 (4.7)	8.4 (8.8)	18.1 (18.5)	-	4.9	-	1.80	-	-	-
[Co(L <sub>4</sub> )(OAc) <sub>2</sub> (H <sub>2</sub> O) <sub>2</sub> ].H <sub>2</sub> O/ IV	>300 Dark Red	45.1 (45.1)	4.8 (5.2)	9.4 (9.6)	10.8 (10.1)	-	5.0	-	2.25	2.05	2.19	2.10

**Table 2: Significant IR and electronic absorption data of oxaloyldihydrazones and their cobalt(II) complexes.**

Symbol	v(OH) phenolic (enolic)	v(H <sub>2</sub> O)	v(NH)	v(C-H) aromatic (aliphatic)	v(C=O)	v(C=N)	v(C-O) phenolic	v(C-OMe)	v(C=C)	δ(C-H) aromatic out of plane	v(M-O) phenolic/enolic (carbonyl/methoxy)	λ <sub>max</sub> , (nm) (assignments)
<b>L<sub>1</sub></b>	3149 (3278)	-	3204 (2924)	3062	1666	1620	1275	-	1403 1458 1486	756	-/- (-/-)	387(n-π*, C=N), 372(n-π*, C=O), 340(π-π*, C=N), 300(π-π*, C=O), 288(π-π*, Phenyl)
<b>L<sub>2</sub></b>	3476 (-)	-	3166 (2926)	3043 1660	1705	1621	1287	-	1465 1541 1574	741	-/- (-/-)	395(n-π*, C=N), 390(n-π*, C=O), 370(π-π*, C=N), 348(π-π*, C=O), 320(π-π*, Phenyl)
<b>L<sub>3</sub></b>	3448 (-)	-	3293 (2923)	3048 1651	1689	1607	1246	-	1449 1486 1512	746	-/- (-/-)	378(n-π*, C=N), 348(n-π*, C=O), 322(π-π*, C=N), 300(π-π*, C=O), 280(π-π*, Phenyl)
<b>L<sub>4</sub></b>	- (3227)	-	3202 (2940)	3041	1653	1600	-	964	1464 1486 1572	760	-/- (-/-)	371(n-π*, C=N), 345(n-π*, C=O), 320(π-π*, C=N), 290(π-π*, C=O), 270(π-π*, Phenyl)
<b>I</b>	- (3278)	3362	3204	3062 (2925)	1666	1604	1303	-	1405 1467	757	532/- (-/-)	500 ( <sup>4</sup> T <sub>1g</sub> → <sup>4</sup> T <sub>1g</sub> (P)), 700 ( <sup>4</sup> T <sub>1g</sub> → <sup>4</sup> A <sub>2g</sub> ) 450(L→MCT)
<b>II</b>	- (-)	3393	3175	3056 (2927)	1654	1618 1601	1303	-	1457 1538	747	520/463 (-/-)	500 ( <sup>4</sup> T <sub>1g</sub> → <sup>4</sup> T <sub>1g</sub> (P)), 700 ( <sup>4</sup> T <sub>1g</sub> → <sup>4</sup> A <sub>2g</sub> ) 450(L→MCT)
<b>III</b>	- (-)	3418	3290	3077 (2931)	1631	1610 1580	1309	-	1445 1489	749	555/478 (-/-)	515 ( <sup>4</sup> T <sub>1g</sub> → <sup>4</sup> T <sub>1g</sub> (P)), 690 ( <sup>4</sup> T <sub>1g</sub> → <sup>4</sup> A <sub>2g</sub> ) 450(L→MCT)
<b>IV</b>	- (3227)	3400	3202	3041 (2939)	1653	1600	-	963	1464 1488	760	-/- (-/-)	515 ( <sup>4</sup> T <sub>1g</sub> → <sup>4</sup> T <sub>1g</sub> (P)), 685 ( <sup>4</sup> T <sub>1g</sub> → <sup>4</sup> A <sub>2g</sub> ) 400(L→MCT)

$L_4$  which has not o-hydroxy group revealed  $\nu(\text{NH})$  at  $3202\text{ cm}^{-1}$  and  $\nu(\text{C}=\text{O})$  at  $1653\text{ cm}^{-1}$ . The appearance of both  $\nu(\text{C}=\text{O})$  and  $\nu(\text{NH})$  simultaneously in the IR spectra of  $L_1$ - $L_4$  refers to the presence of keto forms. The appearance of carbonyl groups ( $\text{C}=\text{O}$ ) near  $1660\text{ cm}^{-1}$  as one band in case of  $L_1$  and  $L_4$  and pair of bands near ( $1660, 1700\text{ cm}^{-1}$ ) for each  $L_2$  and  $L_3$  suggests the presence of  $L_1$  and  $L_4$  in trans (staggered-structure, Fig. 1) configuration while  $L_2$  and  $L_3$  in mixture of [cis(syn/anti-cis-structure) + trans (staggered-structure), Fig.1] isomers. This assumption arises from the field effect phenomenon which can be elucidated as follows. When the two carbonyl ( $\text{C}=\text{O}::$ ) groups are in the same direction (cis configuration), the non-bonding electrons present on oxygen atoms cause electrostatic repulsion. This causes a change in the state of hybridization of  $\text{C}=\text{O}$  group and also makes it to go out of the plane of the double bond. Thus, the configuration diminished and absorption occurs at higher wave number. Subsequently, the cis isomer is absorbed (due to the field effect) at higher frequency compared to trans one. Thereby,  $L_2$  and  $L_3$  showed two bands for  $\text{C}=\text{O}$ , one of them (at high frequency) associated with syn/anti-cis-symmetry while that at lower frequency related to staggered configuration. The low intensity of high frequency bands (near  $1700\text{ cm}^{-1}$ ) compared with that at low frequency (near  $1660\text{ cm}^{-1}$ ) indicates the domination of staggered structure. Worthy mention, NMR spectroscopy is in good agreement with this suggestion. The observation of OH (phenolic) group in  $L_1$  at lower position ( $3149\text{ cm}^{-1}$ ) is taken as evidence to the persistence of intermolecular H-bonding between the phenolic-OH and azomethine group ( $\text{O}-\text{H}\cdots\text{N}$ ) [27]. The proposition of intermolecular H-bond ( $\text{O}-\text{H}\cdots\text{O}-\text{H}$ ) between ligand molecules is excluded owing to the sharpness of this band. The remarkable downward frequency shift indicates the strength of this bond. In fact,  $^1\text{H}$  NMR did not distinguish this H-bond in its spectra because execution of NMR analysis in high polar solvent (DMSO) led to break these bonds. The phenolic-OH group did not form H-bonding in case of ligands  $L_2$  and  $L_3$  where it is observed after  $3400\text{ cm}^{-1}$ . Furthermore, the existence of two bands at  $3278\text{ cm}^{-1}$  ( $L_1$ ) and  $3227\text{ cm}^{-1}$  ( $L_4$ ) may be attributed to  $\nu(\text{OH})_{\text{enolic}}$  in H-bond bonding with azomethine group. The lower shift for these two bands than the normal value asserts the weakness of this bond. The obscure of enolic OH in NMR spectra of  $L_1$  and  $L_4$  may be attributed to the following factors: (1) its lower concentrations, in which minute molecules may change one or two of its  $\text{C}=\text{O}$  groups into enolized configuration but the keto form is still dominated, (2) dilution by high polar DMSO disrupted these H-bonds returning the modified molecules into keto forms. The significant  $\nu(\text{C}-\text{O})$  groups associated with the aromatic ring of the dihydrazones  $L_1$ - $L_4$  were observed at  $1275, 1287, 1246$  and  $964\text{ cm}^{-1}$ , respectively [27]. All of the investigated ligands showed 3-4 bands in the range  $1400$ - $1600\text{ cm}^{-1}$  due to  $\nu(\text{C}=\text{C})$  of the aromatic ring. Also, each ligand exhibited strong band in the region  $700$ - $800\text{ cm}^{-1}$  corresponding to the out of plane deformation of the aromatic ring. The positions of other bands assigned to  $\nu(\text{CH})_{\text{aliphatic}}$  near  $2900\text{ cm}^{-1}$  and  $\nu(\text{CH})_{\text{aromatic}}$  near  $3050\text{ cm}^{-1}$  are demonstrated in Table 2.

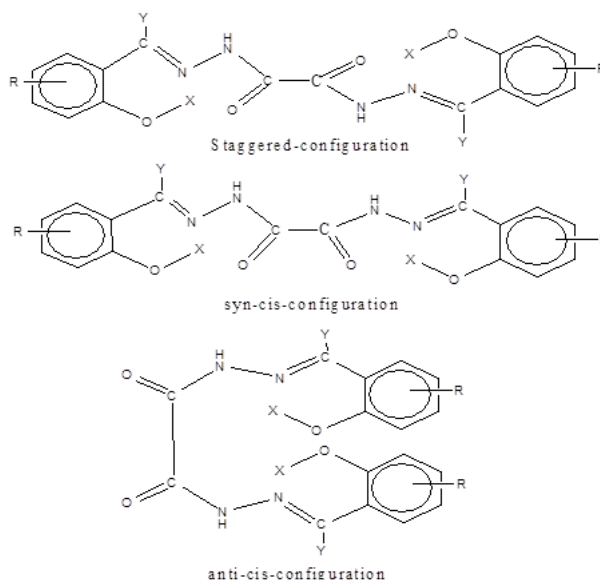


**Fig. 1. Proposed structures of oxaloyldihydrazone ligands, Where  $L_1$  ( $\text{R}=\text{H}$ ,  $\text{X}=\text{H}$ ,  $\text{Y}=\text{H}$ ),  $L_2$  ( $\text{R}=\text{ph}$ ,  $\text{X}=\text{H}$ ,  $\text{Y}=\text{H}$ ),  $L_3$  ( $\text{R}=\text{H}$ ,  $\text{X}=\text{H}$ ,  $\text{Y}=\text{CH}_3$ ) and  $L_4$  ( $\text{R}=\text{H}$ ,  $\text{X}=\text{CH}_3$ ,  $\text{Y}=\text{H}$ ).**

**Co(II) complexes:** The IR spectral data for these complexes pointed out that the dihydrazone ( $L_1$ - $L_4$ ) may act as bi- or tetra-hexadentate ligand toward the centered cobalt ions. The following evidences support this criteria

(Table 2) where: (1) the negative shift of the azomethine group to lower wavenumber in case of I and IV asserted the involvement of this group in bonding [28]. The negative shift of  $\nu(\text{C}=\text{N})$  is attributed to a decrease in the  $\pi$ -bond character of the  $-\text{C}=\text{N}$  group as a result of nitrogen to metal coordination. The splitting in the vibrational stretching  $\text{C}=\text{N}$  band remarked in II and III complexes substantiated the presence of two dissimilar azomethine groups [29] as shown later in Fig. 4. This occurred due to enolization of the left or right half of the dihydrazone molecule assuming keto-enol skeleton. (2) Appearance of both  $\nu(\text{NH})$  and  $\nu(\text{C}=\text{O})$  after chelation (in case of I and IV) at nearly the same positions without any shift indicated that their corresponding ligands coordinate in keto form. The observation of  $\nu(\text{NH})$  and  $\nu(\text{C}=\text{O})$  of II and III as weak bands is due to the obscure of one NH and one C=O groups by virtue of enolization effect. Foundation of C=O as one band in case of II and III complexes instead of two bands in relevant free ligands besides its absorption at somewhat low frequency is most probable due to (a) the presence of the two carbonyl oxygen in trans direction because of the field effect (as in the structure of complex II, Fig. 4) or (b) the presence of the two carbonyl oxygen in cis direction but the electrons of carbonyl/enolized oxygen are occupied in coordination with the central metal ion (as in the configuration of complex III, Fig. 4). (3) Unnoticeable of o-hydroxyl group ( $\nu(\text{OH})_{\text{phenolic/naphthoic}}$ ) reflected the deprotonation of this group during the coordination as in case of I-III species. This result is also confirmed by the appearance of the new band attributed to metal-oxygen bond,  $\nu(\text{M}-\text{O}_{\text{phenolic/naphthoic}})$ , as well as the positive shift observed for  $\nu(\text{C}-\text{O})$  vibrations [27,10]. The observation of  $\nu(\text{M}-\text{O}_{\text{enolic}})$  [30] in II and III at 463 and 478  $\text{cm}^{-1}$ , respectively, explicated the deprotonation of enolic OH in ligands  $\text{L}_2$  and  $\text{L}_3$  upon chelation with Co(II) ion. Besides, the existence of  $\nu(\text{C}-\text{OMe})$  in IV at the same frequency (compared with free  $\text{L}_4$  ligand) without appearance of  $\nu(\text{M}-\text{O}_{\text{methoxy}})$  ruled out the involvement of methoxy oxygen in coordination. (4) The two bands observed at 1345–1381 and 1404–1436  $\text{cm}^{-1}$  in II-IV complexes refer to  $\nu_{\text{as}}$  and  $\nu_{\text{s}}$  carboxylic modes respectively, elucidating the presence of acetate ion in the proposed structures (Fig. 4). The larger separation between the  $\nu_{\text{as}}$  and  $\nu_{\text{s}}$  frequencies confirmed the coordination of acetate as a unidentate anion through the C-O moiety of the carboxylic group [31]. Moreover, strong broad absorptions in the range 3300–3500  $\text{cm}^{-1}$  (Table 2) for all complexes suggested the presence of crystalline or coordinated water. The slight changes in the positions of  $\nu(\text{C}=\text{C}_{\text{ph}})$  upon chelation arises from the metal-ligand interaction.

### $^1\text{H}/^{13}\text{C}$ NMR Spectra

The assignment of the main signals in  $^1\text{H}$  NMR spectra of four ligands [11] are given in Table 1, where cobalt complexes have not been scanned owing to their paramagnetic nature.  $^1\text{H}$  NMR spectra of all ligands exhibited multiple signals of the aromatic protons in the 6.5–8.5 ppm region. The signals of equal integration observed in  $\text{L}_1$ ,  $\text{L}_2$  and  $\text{L}_3$  at  $\delta$  (12.6, 11), (12.8, 12.6) and (12.9, 11.8) ppm downfield of TMS have been assigned to NH and ortho-OH protons, respectively. On the other hand,  $\text{L}_4$  revealed a signal at 12.3 ppm attributed to secondary NH group. Addition of  $\text{D}_2\text{O}$  led to obscure OH and NH signals. Further, the existence of the  $\delta\text{OH}$  (phenolic/naphthoic) at its normal frequency confirmed that ortho-OH did not establish intramolecular hydrogen bonding with  $\text{CH}=\text{N}$  group. The azomethine signals,  $\delta(\text{CH}=\text{N})$ , observed only in  $\text{L}_1$ ,  $\text{L}_2$  and  $\text{L}_4$  have been assigned at 8.75, 9.73 and 8.95 ppm, respectively. As reported in the literature [30], if the dihydrazone exists in the syn-cis-configuration or staggered configuration, the  $\delta\text{OH}$ ,  $\delta\text{NH}$  and  $\delta\text{CH}=\text{N}$ , resonances, each should appear as a singlet. However, the appearance of these signals in the form of six signals (doublet of doublet) indicates anti-cis (chair) configuration. Actually, the features of the  $^1\text{H}$ -NMR spectra of the dihydrazones are in consistent with the syn-cis- or staggered configuration. According to IR interpretation mentioned above, the staggered configuration is well defined/dominated for all ligands ( $\text{L}_1$ - $\text{L}_4$ ).  $^1\text{H}$  NMR spectra of  $\text{L}_3$  and  $\text{L}_4$  differed from other ligands spectra where they showed signals at 2.55 and 3.9 ppm downfield of TMS assigned to the methyl ( $\text{CH}_3$ ) and methoxy ( $\text{OCH}_3$ ) protons, respectively [8,11,31].

The  $^{13}\text{C}$  NMR measurement was checked for  $\text{L}_2$  (synonymous to  $\text{L}_1$  and  $\text{L}_3$ ) and  $\text{L}_4$  ligands where the resulting data (Fig. 2) correlate well with  $^1\text{H}$  NMR spectra without discrepancies. The  $^{13}\text{C}$  NMR spectroscopy data for  $\text{L}_2$  gave resonances at 155.7 ppm for C=O, 149.7 ppm for C=N and 158.3, 132.5, 128.9, 127.8, 123.6 for Ar-C2, Ar-C4, Ar-C6, Ar-C5, Ar-C1, respectively, confirming a staggered symmetry for  $\text{L}_2$ . The greater number of lines than the carbon types in the proposed configuration may be recognized from the existence of some ligand molecules in diketo and/or dienol forms.  $^{13}\text{C}$  NMR spectrum of  $\text{L}_4$  was also in good conformance with  $^1\text{H}$  NMR assuming a keto-keto form (staggered structure). The spectrum showed three peaks assigned to C=O (156.2 ppm), C=N (148.7 ppm) and  $\text{OCH}_3$  (55.7 ppm). The peaks at 158.1, 132.1, 125.8, 122.0, 120.9 are due to Ar-C2, Ar-C4, Ar-C6, Ar-C5, Ar-C1, respectively. The signals observed in-between 25-50 ppm is attributed to the used solvent (DMSO).

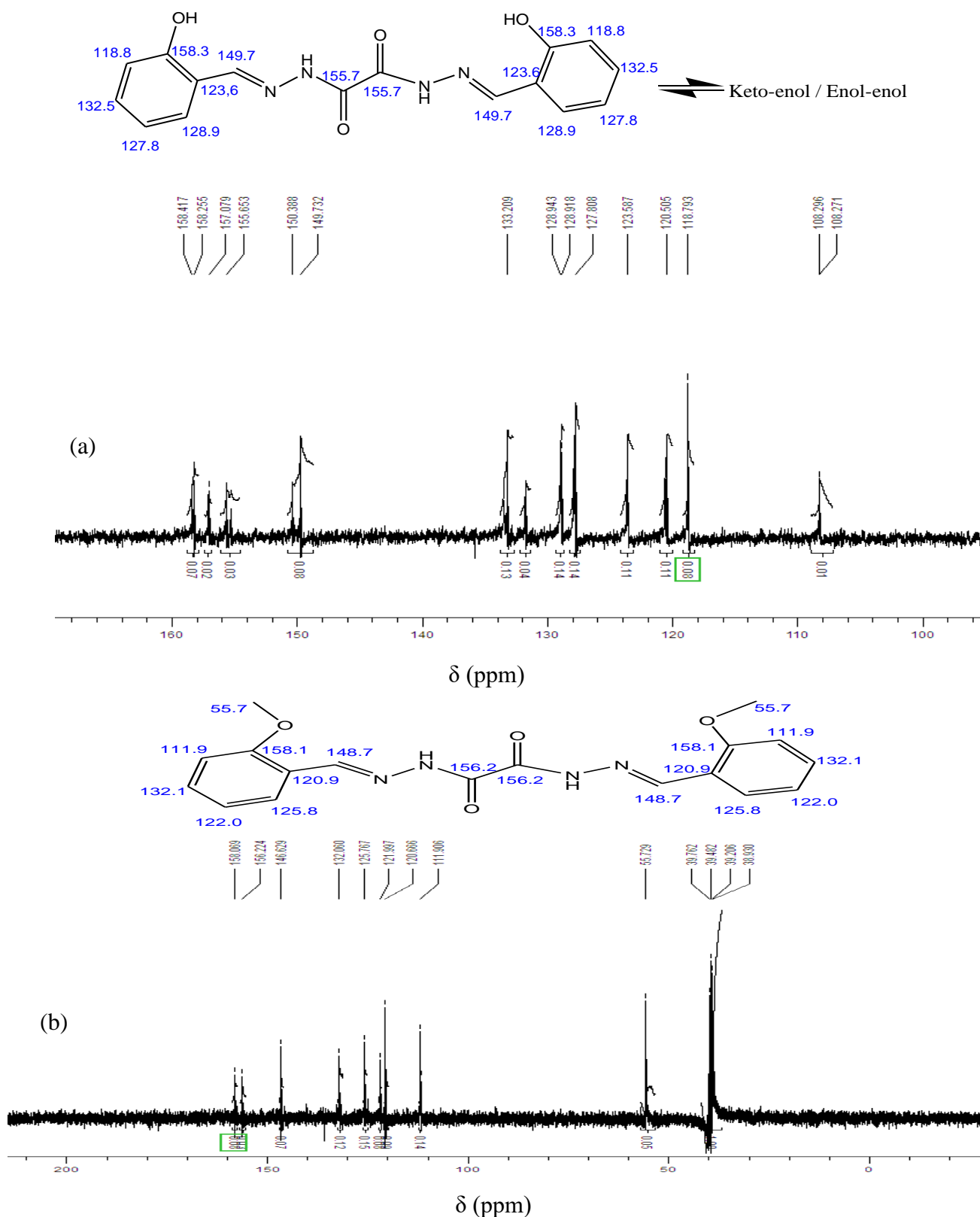


Fig. 2. <sup>13</sup>C NMR spectra of L<sub>2</sub> (a) and L<sub>4</sub> (b) in DMSO-*d*<sub>6</sub> at RT.

### Electronic spectra

The assignments of the observed electronic absorption bands of the oxaloylhydrazones and their metal complexes as well as the magnetic data of the formed chelates are depicted in Table 2.

The electronic data of the studied ligands in Nujol mull exhibited five absorption bands at  $\lambda_{\max}$  (nm) equals 371-390 ( $n-\pi^*$ , C=N), 345-390 ( $n-\pi^*$ , C=O), 320-370 ( $\pi-\pi^*$ , C=N), 290-348 ( $\pi-\pi^*$ , C=O) and 270-320 ( $\pi-\pi^*$ , aromatic ring) [13, 14]. All the Co<sup>II</sup>-complexes in Nujol mull showed two bands at 580-700 and 500-530 nm (Table 2) attributed to  ${}^4T_{1g} \rightarrow {}^4A_{2g}$  (P) and  ${}^4T_{1g} \rightarrow {}^4T_{1g}$  (P) transitions, respectively, considering octahedral structures [32,33]. The complexes showed also another bands in the visible region at 430-450 nm. Since dihydrazone ligands is not expected to be chromophoric in the visible region and all the complexes (I, II, III, and IV) are paramagnetic, these bands have been assigned as the ligand–metal charge transfer (L→MCT) transition on the basis of their high intensity. They may be associated, most probably, with a ligand-to-metal charge transfer originating from an electronic excitation from the HOMO of ortho phenolate/naphtholate/methoxy oxygen to the LUMO of cobalt (II) ion [32]. Any band due to d-d transition in this region is masked by this charge transfer transition.

### Magnetic behavior

At room temperature, the values of  $\mu_{\text{eff}}$  (Table 1) in case of complexes I and IV which contain one metal ion are close to spin only values and may be considered in good consistent with the proposed structures. For other consequential binuclear complexes (II, III), the magnetic moment values are less than that expected per molecular formula regarding the existence of two metal ions in the proposed structures. This can be explained on the basis of metal-metal interaction. It is suggested that these complexes have high spin but presence of two metals near to each other in the same molecule may cause partial quenching of the spin moments of the metal ions (spin coupling) decreasing the magnetism [32].

Variation of magnetic susceptibility with temperature in case of all cobalt complexes has been studied. The  $\chi_M$  versus T and  $\mu_{\text{eff}}$  versus T plots are illustrated in Fig. 3. Indeed, change of magnetism with increasing temperatures for all cobalt species may be taken as conclusive evidence for the formation of high spin octahedral complexes where  $\mu_{\text{eff}}$  of the tetrahedral Co(II) complexes is independent of temperature.

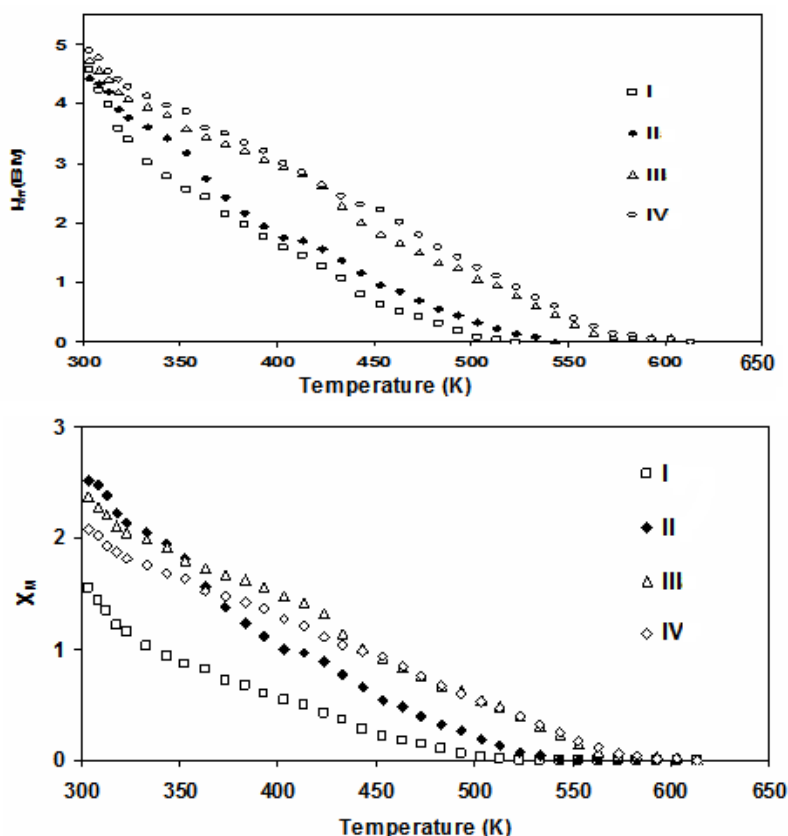


Fig. 3. Temperature variation of the magnetic susceptibility and magnetic moment of Co(II) complexes.

Inspection of figure 3 illustrated that the molar magnetic susceptibility ( $X_M$ ) and effective magnetic moment ( $\mu_{\text{eff}}$ ) for these complexes are minimized slowly with increasing the temperature until reaching zero value of magnetism ( $X_M/\mu_{\text{eff}} = 0$ ). Such behavior is suggested to be characteristic of "normal" paramagnetic behavior of Co(II) complexes and can be interpreted as follows. Upon enhancing the temperature from 300 to 650 K and in the presence of air, some molecules of high spin octahedral Co(II) complexes varied their spin state gradually from ( $t_{2g}^5 e_g^2$ ) to ( $t_{2g}^6 e_g^0$ ) converting to low spin Co(III) octahedral complexes. This modification was prolonged until all the Co(II) complexes have been oxidized completely by heat/oxygen into analogous Co(III) complexes. Thereby, the magnetism becomes zero where all the complexes molecules accepted diamagnetic nature.

### TG studies of Co(II)-complexes

Thermal stability for some complexes (III, IV) was studied and can be taken as indication for other analogous complexes. The thermogram (TGA) data of complex (III) exhibited three stages of decomposition. The first stage (50-120 °C) corresponds to the loss of one uncoordinated acetate group (found/calculated % = 8.31/8.95), the second step of decomposition (140-340 °C) may be due to elimination of six coordinated water molecules (found/calculated % = 16.49/16.97), meanwhile the third stage refers to the decomposition of the complex with formation of 2CoO as final product (found/calculated % = 24.65/23.75). The TGA data of complex (IV) revealed four stages of decomposition. The first one concerns the loss of 2.42 % of the weight at temperature range from (50-150 °C) corresponding to the removal of one crystalline water molecule (calculated % = 3.0). The second step of decomposition, 150-250 °C, refers to the loss of two coordinated water molecules (found/calculated % = 5.56/6.0). The third stage observed at 250-360 °C points to the loss of two acetate groups (found/calculated % = 20.4/19.5). Finally, the fourth stage is related to the decomposition of the complex with formation of  $\text{CoCO}_3$  (found/calculated % = 19.4/20.3) as final product.

In view of data presented and discussed above, structures of the cobalt(II) complexes can be represented by Fig. 4.

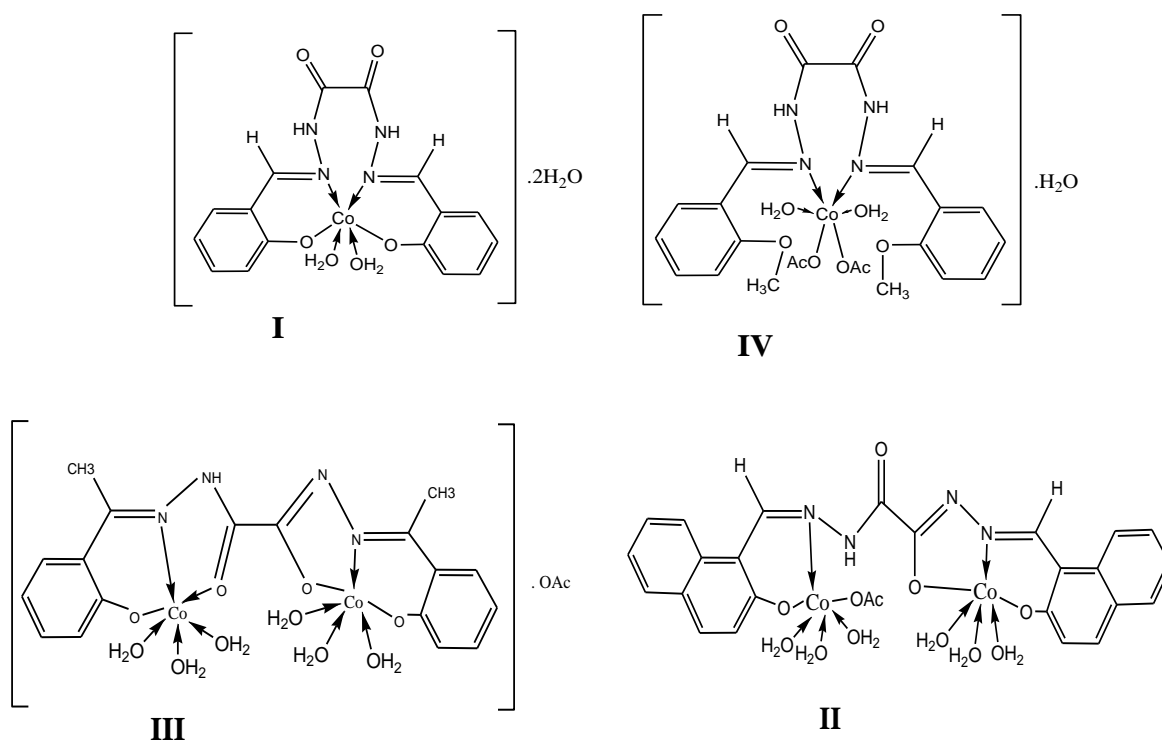


Fig. 4. Suggested structures of the Co<sup>II</sup>-oxaloyldihydrazone complexes.

## ESR Spectra

The Co(II) complexes give poorly resolved ESR spectra at room temperature, even though it is a  $d^7$  system. The Co(II) ( $d^7$ ) ion is being a non-Krammer's ion and its ESR spectrum is observable, generally at low temperatures. However, there are very few reports in the literature about the study of this  $d^7$  ion at room temperature. Most of the reported work concerns the study of this ion at 77 K or 4 K. There are a few extra resonance lines, which might have been arisen from forbidden transitions. ESR spectra of I, II and IV complexes revealed broad signals with hyperfine splitting (Fig. 5). The obtained  $g$  values ( $g_{//}$ ,  $g_{\perp}$ ) are depicted in Table 1. The average  $g$  values were calculated according to the following relation:

$$g_{av.} = \frac{1}{3[g_{//} + 2g_{\perp}]}$$

where, the calculated  $g_{av}$  values are inserted also in Table 1.

The  $g_{//}$  is a moderately function for covalent character. The complexes I, II and IV exhibited  $g_{//}$  at 2.40, 2.23 and 2.19, respectively suggesting covalent nature of cobalt - ligand bond in I and ionic character for II and IV. where,  $g_{//} > 2.3$  is character of ionic metal - ligand bond while  $g_{//} < 2.3$  describes covalent metal - ligand interaction [33]. Fairly high values of  $g$  are in conformity with the oxygen and nitrogen coordination in these compounds [35]. The hyperfine splitting in the investigated Co(II) complexes is probably due to dissimilar bonds associated with the positive Co(II) ion or arises from the effect of the magnetic moment of the ligand nuclei on the metal unpaired electrons [36].

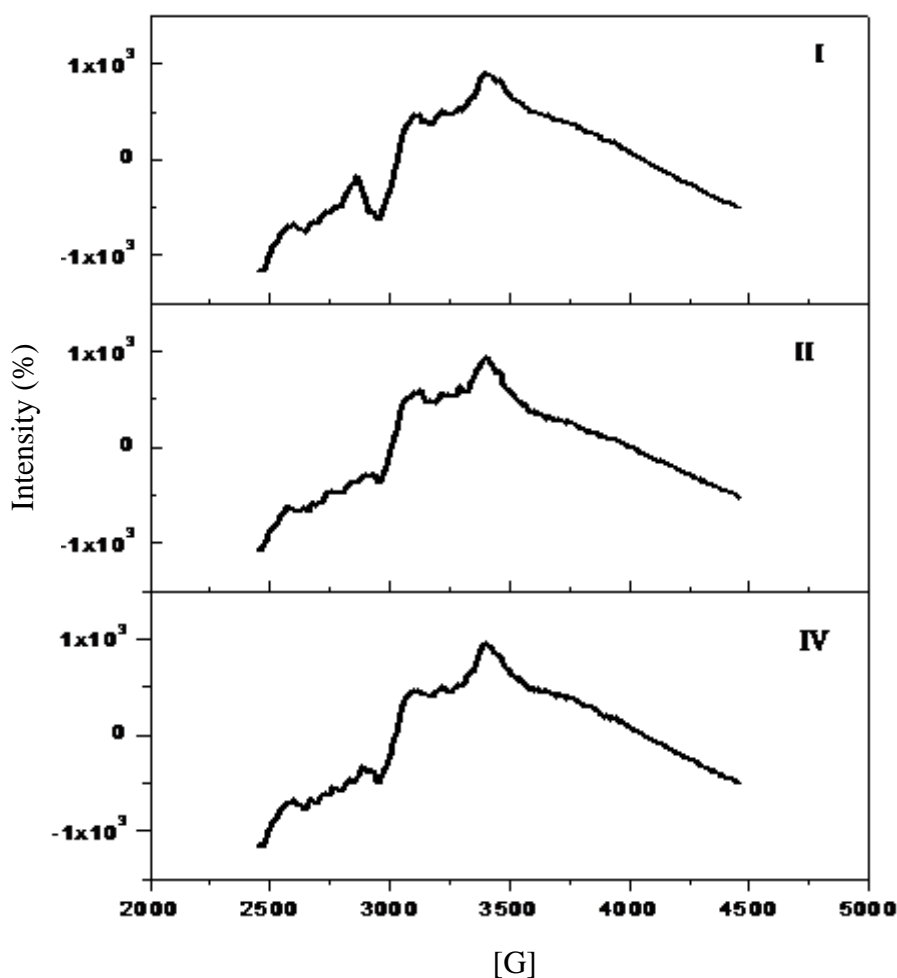


Fig. 5. ESR spectra of solid Co<sup>II</sup>-oxaloyldihydrazone complexes.

### Optical properties

To clarify the conductivity of the isolated complexes, the optical band gap energy ( $E_g$ ) of oxaloyldihydrazones and their Co(II) complexes have been calculated from the following equations [23,24,11]:

The measured transmittance (T) was used to calculate approximately the absorption coefficient ( $\alpha$ ) using the relation

$$\alpha = \frac{1}{d \ln(1/T)}$$

where d is the width of the cell and T is the measured transmittance. The optical band gap was estimated using Tauc's equation:

$$\alpha h\nu = A(h\nu - E_g)^m$$

Where m is equal to 1/2 and 2 for direct and indirect transitions, respectively, and A is an energy independent constant.

The values of  $\alpha$  calculated from the first equation were used to plot  $(\alpha h\nu)^2$  vs.  $h\nu$  (Fig. 6) from which an indirect band gap was found by extrapolating the linear portion of the curve to  $(\alpha h\nu)^2 = 0$ . The values of

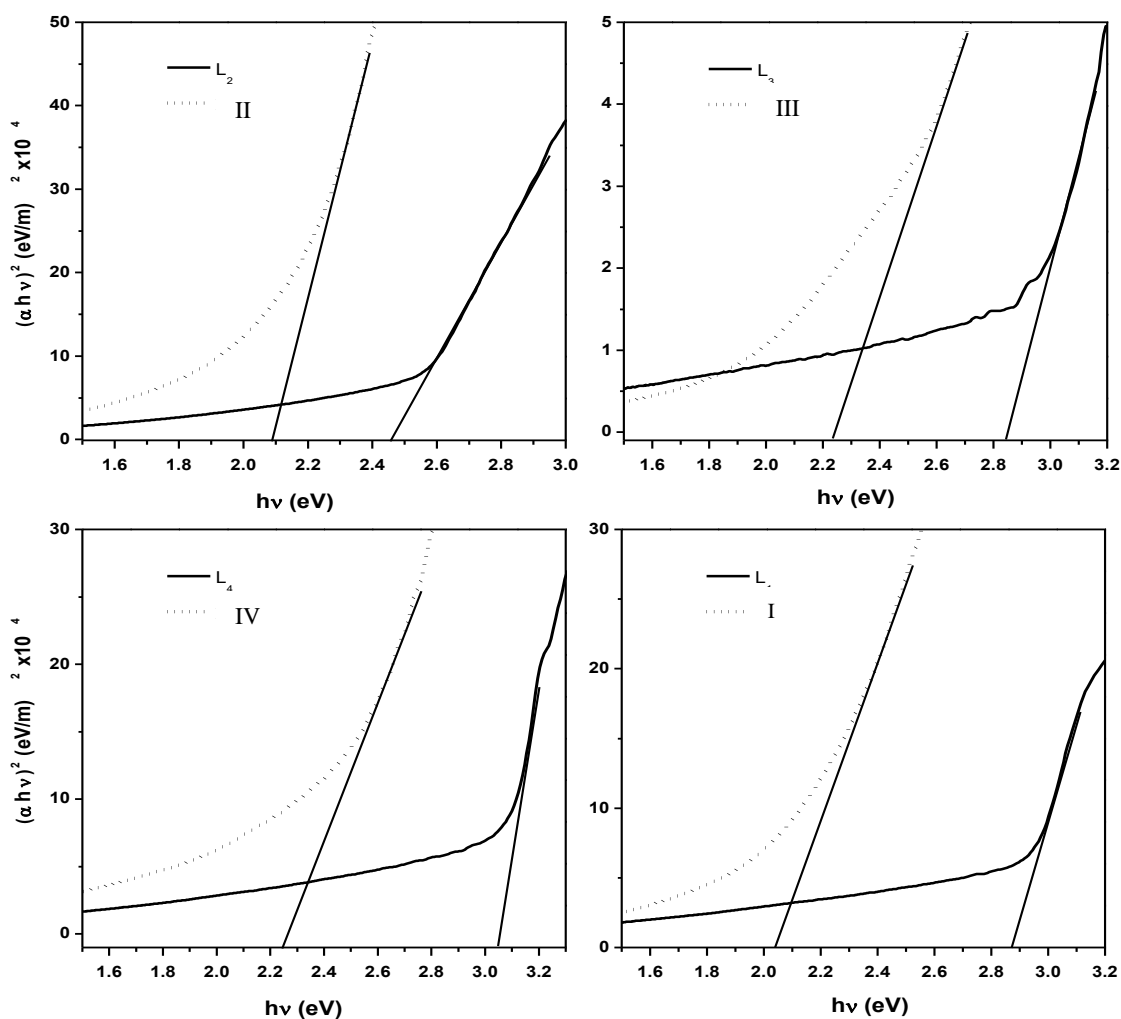


Fig. 6. The plots of  $(\alpha h\nu)^2$  vs.  $h\nu$  of Co<sup>II</sup>-oxaloyldihydrazone complexes.

indirect optical band gap  $E_g$  were determined and are given in Table 1. The  $E_g$  values of oxaloyldihydrazones (**L<sub>1</sub>-L<sub>4</sub>**) and Co(II)-L complexes were found to be at 3.06-3.42 and 1.80-2.25 eV, respectively as indicated in Fig. 6 and Table 1. Inspection of Table 1 revealed higher  $E_g$  values of ligands compared with their corresponding complexes. As reported in the literature [37] it is suggested that after complexation, metal leads to raise mobilization of the ligand electrons by accepting them in its shell. It can be evaluated that after formation of the complex, the chemical structure of the ligands is changed, the width of the localized levels is expanded and in turn, the band gap is smaller. This result is very significant in applications of electronic and optoelectronic devices, because of the lower optical band gap of the materials [38]. Worthy mention, small band gap facilitates electronic transitions between the HOMO-LUMO energy levels and makes the molecule more electro-conductive [39]. The obtained band gap values suggest that these complexes are semiconductors and lay in the same range of highly efficient photovoltaic materials. So, the present compounds could be considered potential materials for harvesting solar radiation in solar cell applications [37,40]. The little difference in the optical band gap  $E_g$  values between all studied complexes may be due to their synonymous chemical structures.

### Anti-tumor Activity

Inhibitory activity of Co(II)-oxaloyldihydrazone complexes against breast carcinoma cells (MCF-7 cells) was detected with cell viability values demonstrated in Fig. 7. The results showed that the two compounds I and II have lower inhibitory activities against breast carcinoma cells than compounds III and IV which possess inhibitory activities with  $IC_{50}$ = 24.9 and  $IC_{50}$ =37.7  $\mu$ g/ml respectively. For comparison purposes, the cytotoxicity of Vinblastine (structure 1), as standard anti-tumor drug, was evaluated and produced  $IC_{50}$  value (4.6  $\mu$ g/ml) under the same conditions.

Toxicity of the compounds III and IV was evaluated against normal cells (African Green Monkey Kidney, VERO cells) and the cell viability values are shown in Fig. 8. The two compounds III and IV revealed activation with  $IC_{50}$ = 36.7 and  $IC_{50}$ =39.1  $\mu$ g/ml respectively. The toxicity of these complexes could be interpreted based on their greater solubility and lipophilicity. The lipophilicity increases with increasing bulkiness and may facilitate transport through the cellular membrane [41].

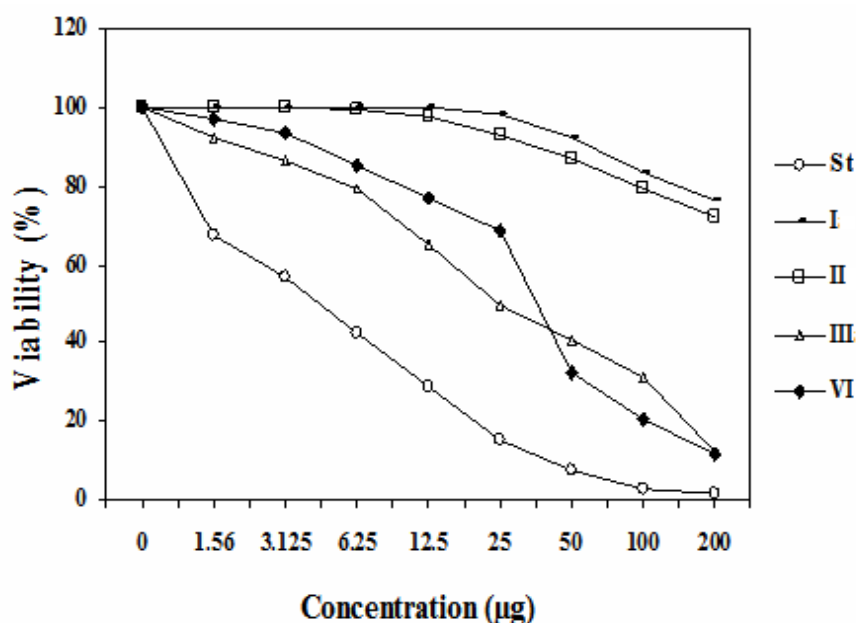


Fig. 7. Chart of evaluation of cytotoxicity against MCF-7 cell line for Co(II) complexes.

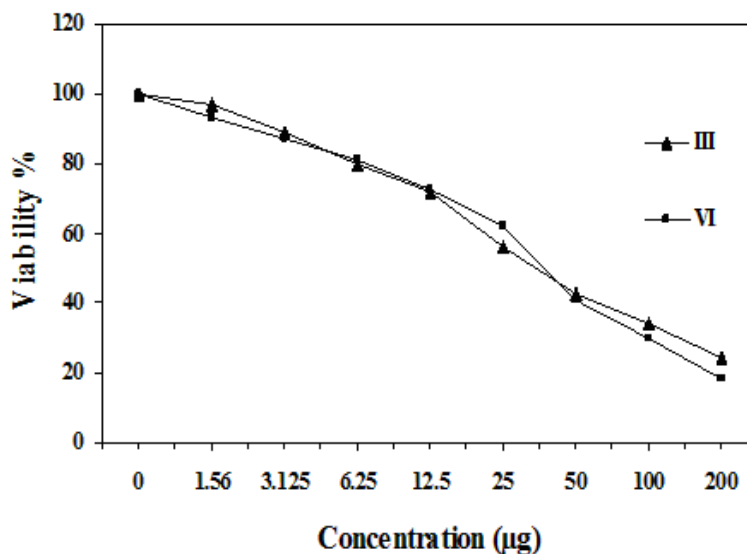
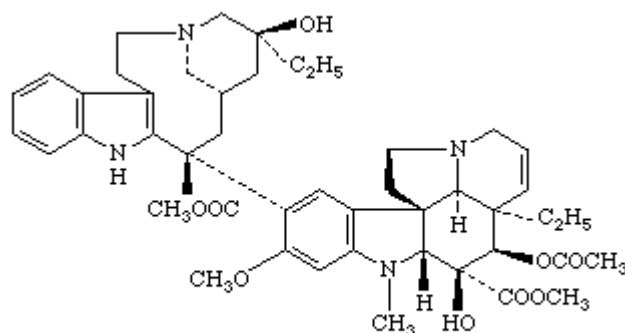


Fig. 8. Chart of evaluation of cytotoxicity against VERO cell line for III and IV complexes.



Structure 1. Vinblastine structure

## CONCLUSION

A series of cobalt(II)-hydrazone complexes derived from some selected oxaloyldihydrazones (L<sub>1</sub>-L<sub>4</sub>) have been isolated in pure form. All the ligands and their four solid cobalt(II) complexes may be prepared by conventional reflux method. Comparison of the elemental analysis for both calculated and found percentages indicates that the compositions of the isolated solid complexes coincide well with the proposed formulae. Elemental analyses (C, H, N and M%), FT-IR, UV-Vis and ESR spectroscopy, thermal measurement, magnetism at different temperature besides the difference in the color between the free ligand and its corresponding complex evidenced the formation of the desired cobalt-hydrazone complexes. The dihydrazones give mononuclear complexes with L<sub>1</sub> and L<sub>4</sub> but binuclear complex is formed with L<sub>2</sub> and L<sub>3</sub>. The cobalt center in all separated complexes prefers an octahedral configuration. The indirect band gap energies (E<sub>g</sub>) for all ligands and complexes lie in the range of semiconductor materials. The investigated compounds were assayed for their anti-tumor activities against the human breast cancer cell line. The results suggested that the Co(II)-complexes have growth inhibition activity. The toxicity of the compounds III and IV against the African Green Monkey Kidney (VERO cells) were evaluated and the results demonstrated that the two compounds III and IV

have activity with  $IC_{50} = 36.7$  and  $IC_{50} = 39.1$   $\mu\text{g/ml}$  respectively. The activity of these complexes could be explained by their greater solubility and lipophilicity.

#### REFERENCES

- [1] Barbazan P, Carballo R, Covelo B, Lodeiro C, Lima JC, Vazquez-Lopez EM, *Eur J Inorg Chem* 2008; 2713–2720.
- [2] Kabil MA, Ghazy SE, Mostafa MA, El-Asmy AA, *Fresenius J Anal Chem* 1994; 349: 775–776.
- [3] Salem AA, *Microchem J* 1998; 60: 51–66.
- [4] Dass R, Mehta JR, *Indian J Chem* 1994; 33: 438–439.
- [5] Fujimoto T, Teshima N, Kurihara M, Nakano S, Kawashima T, *Talanta* 1999; 49: 1091–1098.
- [6] Berger SA, *Microchem J* 1993; 47: 317–324.
- [7] Berger SA, *Mikrochim Acta* 1984; 84: 275–282.
- [8] Sherif EM, Ahmed AH, *Synth React Inorg Met-Org Chem* 2010; 40: 365–372.
- [9] Ghasemian M, Kakanejadifard A, Azarbani F, Zabardasti A, Shirali S, Saki Z, Kakanejadifard S, *Spectrochim Acta* 2015; 38: 643–647.
- [10] Ahmed AH, Ewais E, *J Chem Pharm Res* 2012; 4: 3349–3360.
- [11] Hassan AM, Ahmed AH, Gumaa HA, Mohamed BH, Eraky AM, *J Chem Pharm Res* 2015; 7: 91–104 and references therein.
- [12] Yuan J, Lovejoy DB, Richardson DR, *Blood* 2004; 104: 1450–1458.
- [13] Bhaskar R, Salunkhe N, Yaul A, Aswar A, *Spectrochim Acta* 2015; 151: 621–627.
- [14] Ahmed AH, Hassan AM, Gumaa HA, Mohamed BH, Eraky AM, *Cogent Chem* 2016; 2: 1142820.
- [15] Ahmed AH, Hassan AM, Gumaa HA, Mohamed BH, Eraky AM, Omran AA, *Arab J Chem* 2016, In press.
- [16] Lal RA, Basumatary D, Adhikari S, Kumar A, *Spectrochim Acta A* 2008, 69: 706–714.
- [17] (a) Ahmed AH, *Rev Inorg Chem* 2014; 34: 153–175. (b) Ahmed AH, Thabet MS, *J Mol Struct* 2011; 1006: 527–535.
- [18] Kratz F, Beyer U, Roth T, Tarasova N, Collery P, Lechenault F, Cazabat A, Schumacher P, Unger C, Falken U, *J Pharm Sci* 1998; 87: 338–346.
- [19] Datta A, -Hsin Liu P, -Hsien Huang J, x Garribba J, Turnbull M, Machura B, -Lin Hsu C., -Tang Chang W, Pevec A, *Polyhedron* 2012; 44: 77–87.
- [20] Sharma VK, Srivastava S, *Synth React Inorg Met-Org Nano-Met Chem* 2005; 35: 311–318.
- [21] Hoonur RS, Patil BR, Badiger DS, Vadavi RS, Gudasi KB, Dandawate PR, Ghaisas MM, Padhye SB, Nethaji M, *Eur J Med Chem* 2010; 45: 2277–2282.
- [22] Ahmed AH, Thabet MS, *Syn. and Rea in Ino and Metal-Org. Chem* 2015; 45: 1632–1641.
- [23] Rashad MM, Hassan AM, Nassar AM, Ibrahim NM, Mourtada A, *Appl Phys A* 2013; 117: 877–890.
- [24] Tauc J, *Mater Res Bull* 1968; 3: 37–46.
- [25] Ahmed AH, Hassan AM, Gumaa HA, Mohamed BH, Eraky AM, *J Adv in Chem* 2015; 11: 3834–3847 and references therein.
- [26] Mosmann T, *J Immunol Methods* 1983; 65: 55–63.
- [27] Chanu OB, Kumar A, Ahmed A, Lal RA, *J Mol Struct* 2012; 1007: 257–274.
- [28] Ali AM, Ahmed AH, Mohamed TA, Mohamed BH, *Transit Met Chem* 2007; 32: 461–467.
- [29] Salapathy S, Sahoo B, *J Inorg Nucl Chem* 1970; 32: 2223–2227.
- [30] Kumar A, Lal RA, Chanu OB, Borthakur R, Koch A, Lemtur A, Adhikari S, Choudhury S, *J Coord Chem* 2011; 64: 1729–1742.
- [31] Nakamoto K, *Inorganic Spectra of Inorganic and Coordination Compounds*, 2Ed, John Wiley & Sons, New York, 1970.
- [32] Abd El-Wahab H, Abd El-Fattah M, Ahmed AH, Elhenawy AA, Alian NA, *J Organomet Chem* 2015; 791: 99–106.
- [33] Sutton D, *Electronic Spectra of Transition Metal Complexes*, McGraw Hill, London, 1968.
- [34] Lever ABP, *Inorganic Electronic Spectroscopy*, Elsevier Publishing Company, Amsterdam, 1984.
- [35] McCollum DG, Hall L, White C, Ostrandor R, Rheingold AL, Whelan J, Bosnich B, *Inorg Chem* 1994; 33: 924–933.
- [36] Lal RA, Basumatary D, Adhikari S, Kumar A, *Spectrochim Acta A* 2008; 69: 706–714.
- [37] Carrington A, MacLachlan AD, *Introduction to Magnetic Resonance*, Haper&Row, New York, 1967, pp. 167–171.
- [38] Karipcin F, Dede B, Caglar Y, Hur D, Ilcan S, Caglar M, Sahin Y, *Opt Commun* 2007; 272: 131–137.
- [39] Turan N, Gündüz B, Körkoca H, Adigüzel R, Çolak N, Buldurun K, *J Mex Chem Soc* 2014; 58: 65–75.



- [40] Sengupta SK, Pandey OP, Srivastava BK, Sharma V, *Transit Met Chem* 1998; 23: 349–353.  
[41] Fu ML, Guo GC, Liu X, Cai LZ, Huang JS, *Inorg Chem Commun* 2005; 8: 18–21.  
[42] Binks SP, Dobrota M, *Biochem Pharmacol* 1990; 40: 1329–1336.